Structural Origins of Fibrin Clot Rheology

Esther A. Ryan,*§ Lyle F. Mockros,#§ John W. Weisel,¶ and Laszlo Lorand*#

*Department of Cell and Molecular Biology and the #Feinberg Cardiovascular Research Institute, Northwestern University Medical School, Chicago, Illinois 60611; §Department of Biomedical Engineering, Northwestern University, Evanston, Illinois 60208; and the ¶Department of Cell and Developmental Biology, University of Pennsylvania School of Medicine, Philadelphia, Pennsylvania 19104 USA

ABSTRACT The origins of clot rheological behavior associated with network morphology and factor XIIIa-induced cross-linking were studied in fibrin clots. Network morphology was manipulated by varying the concentrations of fibrinogen, thrombin, and calcium ion, and cross-linking was controlled by a synthetic, active-center inhibitor of FXIIIa. Quantitative measurements of network features (fiber lengths, fiber diameters, and fiber and branching densities) were made by analyzing computerized three-dimensional models constructed from stereo pairs of scanning electron micrographs. Large fiber diameters and lengths were established only when branching was minimal, and increases in fiber length were generally associated with increases in fiber diameter. Junctions at which three fibers joined were the dominant branchpoint type. Viscoelastic properties of the clots were measured with a rheometer and were correlated with structural features of the networks. At constant fibrinogen but varying thrombin and calcium concentrations, maximal rigidities were established in samples (both cross-linked and noncross-linked) which displayed a balance between large fiber sizes and great branching. Clot rigidity was also enhanced by increasing fiber and branchpoint densities at greater fibrinogen concentrations. Network morphology is only minimally altered by the FXIIIa-catalyzed cross-linking reaction, which seems to augment clot rigidity most likely by the stiffening of existing fibers.

INTRODUCTION

Fibrinogen is made up of two identical halves, each containing three different peptide chains (Aα, Bβ, and γ) that are held together by a network of disulfide bonds. By electron microscopy the molecule appears as a trinodular structure, having a central domain, consisting of the amino termini of all six chains, and two end domains, whose proximal and distal regions are comprised of the carboxy-terminal ends of the Bβ chains and γ chains, respectively (Weisel et al., 1985). The carboxy-terminal portions of the Aα chain depart from the end domains and fold into a conformation that stretches back toward the central domain (Erickson and Fowler, 1983; Weisel et al., 1985; Veklich et al., 1993; Gorkun et al., 1994).

The conversion of fibrinogen into a network of fibrin fibers occurs through a series of steps. Under physiological conditions, thrombin catalyzes the hydrolytic removal of fibrinopeptides A and B from fibrinogen, converting the molecule to fibrin and revealing binding sites at its central domain that interact with complementary sites at the end domains of other fibrin molecules. These noncovalent interactions cause fibrin monomers to assemble in a half-staggered manner into two-stranded protofibrils. Upon growing to sufficient length, the protofibrils aggregate laterally to form fibers that branch into a three-dimensional network.

Received for publication 4 December 1998 and in final form 9 August 1999.

Address reprint requests to Dr. L. Lorand, Department of Cell and Molecular Biology, Searle 4-555, Northwestern University Medical School, 303 E. Chicago Avenue, Chicago, IL 60611. Tel.: 312-503-0591; Fax: 312-503-0590; E-mail: l-lorand@nwu.edu.

0006-3495/99/11/2813/14 $2.00

The network is further stabilized in the presence of factor XIIIa through the formation of N^{ϵ}-(γ-glutamyl)lysine isopeptide bonds (which are called cross-links or ligations) (Lorand et al., 1968; Matacic and Loewy, 1968; Pisano et al., 1968). Ligations between Lys^{406} and Glu^{398} of the γ-chains of adjacent fibrin molecules result in the formation of γ-dimers (Chen and Doolittle, 1969, 1971; McKee et al., 1970; Doolittle et al., 1971) and γ-multimers (Murthy and Lorand, 1990; Shainoff et al., 1991; Siebenlist and Mosesson, 1992); ligations between the multiple cross-linking sites on the α-chains produce α-polymers (McKee et al., 1970; Schwartz et al., 1971; Sobel et al., 1988; Gron et al., 1992). Factor XIIIa-induced hybrid $\alpha\gamma$-ligations have also been observed (Mosesson et al., 1989; Murthy and Lorand, 1990; Shainoff et al., 1991; Gron et al., 1993).

Covalent cross-linking within fibrin networks produces dramatic effects on clot rheological properties. Ligated clots exhibit mechanical stiffnesses up to five times greater than their unligated counterparts (Ferry et al., 1951; Roberts et al., 1973; Gerth et al., 1974; Mockros et al., 1974; Glover et al., 1975; Shen et al., 1975; Shen and Lorand, 1983) and do not display the stress-induced structural rearrangements seen in unligated clots by creep and by permanent deformation after creep recovery (Nelb et al., 1976, 1981; Janmey et al., 1983). The mechanism by which cross-linking augments clot stiffness remains undetermined. The enhancement of rigidity in ligated clots has been attributed mainly to the development of α-polymers, whereas γ-dimerization is thought to have a smaller (Gladner and Nossal, 1983) or negligible effect (Shen et al., 1974, 1975) on network rigidity.

Early efforts were made (Nelb et al., 1981) to describe the origins of clot rigidity using a model of randomly interpenetrating stiff rods (Doi and Kuzuu, 1980). The network

theory for rubber elasticity was also used to estimate the "cross-linking densities" of clots from their stiffnesses (Ferry and Morrison, 1947; Kaibara and Fukada, 1970; Glover et al., 1975, 1977). Dissimilarities between features of these models and fibrin networks, however, limited their success in identifying the contributions made by the various molecular interactions to clot mechanical behavior.

Clot stiffness is thought to be strongly dependent on fibrin fiber thickness and flexural stiffness, branchpoint density, and fibrin concentration (Roberts et al., 1974; Gerth et al., 1974; Glover et al., 1975; Shen et al., 1975; Nelb et al., 1976). Quantitative correlations between the structural features of clots and their rheology have not been made, partly due to the difficulty of quantitatively analyzing the morphology of the often complex fibrin networks. Qualitative descriptions of network architecture by microscopy under various clotting conditions have been well-documented (Muller et al., 1984; Blomback et al., 1990; Weisel and Nagaswami, 1992; Weisel et al., 1993; Gorkun et al., 1994), and fiber sizes have been estimated using fiber mass to length ratios calculated from light-scattering and permeation techniques (Carr et al., 1977, 1987; Carr and Hermans, 1978; Blomback et al., 1984, 1990; Shah et al., 1985). Direct measurements of clot structural features, however, have been limited.

In the present investigation, extensive quantitative analysis of network features (fiber lengths, diameters, branchpoint densities, and fiber densities) was made using a recently developed method of constructing computerized three-dimensional wire frame models of fibrin networks from stereo electron micrographs (Baradet et al., 1995). Stereo viewing of the networks was particularly useful for measuring fiber lengths in three dimensions and distinguishing branchpoints from fibers that merely crossed each other at different depths. Network structure in clots of purified fibrin was manipulated by varying fibrinogen, thrombin, and calcium ion concentrations, and cross-link formation was controlled through the use of a highly specific, active-center-directed synthetic inhibitor of FXIIIa, 1,3,4,5-tetramethyl-2[(2-oxopropyl)thio]imidazolium chloride (Freund et al., 1994). By measuring clot viscoelastic properties with a cone and plate rheometer and analyzing cross-linking with SDS-PAGE, a correlation was determined between the structural features of the ligated and nonligated clots and their rheology.

MATERIALS AND METHODS

Human fibrinogen (plasminogen free; American Diagnostica, Greenwich, CT) was dissolved in water, dialyzed against 4 l of 50 mM Tris-HCl, pH 7.5, 150 mM NaCl, 1 mM EDTA at 4°C, and stored at −80°C. Protein concentration was determined by absorbance at 280 nm ($E^{1\%}_{1cm}$ = 15.1; Mihalyi, 1968). The commercial fibrinogen was contaminated by small amounts of FXIII, as judged by the detection of bands of α_n and γ–γ cross-linked chains in reducing SDS-PAGE after the fibrinogen (6 μM) had been clotted with human α-thrombin (1 NIHU/ml) and $CaCl_2$ (5 mM) for 90 min at 37°C. Human α-thrombin (a gift from Dr. J. W. Fenton II, New York State Department of Health, Albany, NY) was diluted to 500 NIHU/ml in 50 mM Tris-HCl, 150 mM NaCl, pH 7.5 and stored at −80°C. The synthetic inhibitor of factor XIIIa, 1,3,4,5-tetramethyl-2[(2-oxopropyl)thio]imidazolium chloride (L682777, generously provided by Dr. Andrew Stern, Merck, Sharp and Dohme Research Laboratories, West Point, PA), was dissolved in water and stored at −20°C at a concentration of 100 mM.

Scanning electron microscopy of fibrin clots

Clots were prepared for scanning electron microscopy (SEM) from mixtures that typically contained 0.5–6 mg/ml fibrinogen, 0–5 NIHU/ml thrombin, 0–20 mM $CaCl_2$, 0 or 1 mM inhibitor L682777, 50 mM Tris-HCl (pH 7.5), and sufficient amounts of NaCl (from a stock of 150 mM) to maintain the final ionic strength at 0.15. These reaction components were thoroughly premixed with a pipette tip in 1.5-ml Eppendorf tubes in 120 μl volumes, with thrombin added as a last step to initiate clotting. The mixtures were quickly transferred in volumes of 50 μl from the tube to plexiglass microdialysis cells perforated for solvent perfusion. Clotting proceeded in a moist atmosphere at room temperature (20–22°C) for 2 h. Samples were then fixed, dehydrated, critical point-dried, and sputter-coated according to the methods of Langer et al. (1988). The specimens were washed 3 times by permeation with 50 mM sodium cacodylate-HCl buffer (pH 7.4) to remove excess salt and fixed overnight in 2% glutaraldehyde. Clots were then washed 4 times in distilled water, dehydrated in a graded series of increasing ethanol concentrations (30–100%) over 3.5 h, and critical point-dried with CO_2 in a DCP-1 critical point drying apparatus (Denton Vacuum Co., Cherry Hill, NJ). The specimens were mounted, sputter-coated with gold-palladium in an SEM coating unit E5100 (Polaron Instruments, Inc., West Sussex, England) at 2.2 kV and 20 mA for 1.5 min, and examined in a Philips XL20 scanning electron microscope (Philips Electronics Co., Mahwah, NJ). Duplicates of each clot were made, and several fields on each clot were examined before choosing fields that were characteristic of the entire clot. Digitized electron micrographs were taken at magnifications (between 4000 and 25,000×) that included a relatively high number of branchpoints (>300) and fibers (>500). Stereo pairs were generated by taking pictures in 7.5° increments between −7.5° and 45° by using a tilting, eucentric stage on the microscope.

Computerized three-dimensional reconstructions and quantitative characterization of fibrin networks

Methods of fibrin network analysis were modified from those of Baradet et al. (1995). Digitized scanning electron micrographs were analyzed by custom image analysis software routines written in C by Lou Fodor (Department of Biology, University of Pennsylvania). The images were viewed in stereo with a Crystal Eyes StereoGraphics optical stereo viewer (StereoGraphics Corporation, San Rafael, CA) on a Silicon Graphics Indigo 2 workstation (Silicon Graphics, Inc., Mountain View, CA). Using a series of seven stereo micrograph pairs, the analysis software allowed the three-dimensional specimen images to be viewed and rotated ~45° about a vertical (x) axis. Fiber branchpoints (points at which three or more fibers joined together) were marked directly on the image with a cursor that could be moved in the x-, y-, and z-directions (Fig. 1). Series of several straight links representing fiber segments between the branchpoints were constructed and could be edited to follow the images of the actual fibers in three dimensions.

The complete length of a fiber was defined as the distance measured along the fiber between its terminal branchpoints. Fiber lengths were thus obtained from the reconstructed networks by summing the lengths of the links constructed between branchpoints. In all of the SEM images analyzed in this study, a large number of fibers extended beyond the boundaries of the image before branching or joining with other fibers; therefore, their complete lengths could not be measured. Instead, the lengths of the portions of fibers that could be observed in the image were recorded and considered statistically "censored." These incomplete fiber lengths were

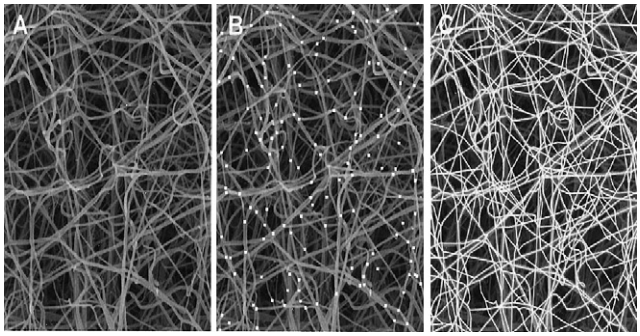

FIGURE 1 Depiction of the process for building three-dimensional network reconstructions. (*A*) Digitized scanning electron micrographs of fibrin networks were viewed in stereo (nonstereo image shown here). (*B*) Branching junctions and endpoints of the fibers were marked on the three-dimensional image, and the *x*-*y*-*z* coordinates of these points were recorded by the image analysis program. (*C*) Series of links representing fibers were constructed between the marked branchpoints or fiber endpoints. The links could be edited to follow the fibers in three dimensions.

included in the analysis of the data, for excluding them would bias the data toward the shorter lengths, particularly in images that included fibers with lengths longer than the dimensions of the image. By using Kaplan-Meier product limit estimates for treating censored data (Kaplan and Meier, 1958), the data were found to fit a gamma distribution from which mean and standard deviations of the fiber lengths were estimated.

Clot fiber diameters were measured directly from high-definition micrographs obtained from the Phillips SEM using public domain National Institutes of Health Image program 1.61 (US National Institutes of Health, Bethesda, MD). Fiber and branchpoint densities were calculated by dividing the total number of fibers and branchpoints measured in the fibrin network models by the volumes taken up by the reconstructions. The presence of incomplete fibers was taken into account in the calculation of fiber densities, assuming that, on average, half the actual (complete) lengths of the incomplete fibers was included inside the network volumes. Estimates of the network volumes were calculated using Matlab software Version 5.0 (The Math Works, Inc., Natick, MA).

Measurement of clot rigidity

A VOR Rheometer (Bohlin Rheologi, Cranbury, NJ) was used to examine the viscoelastic properties of clots having compositions identical to those analyzed by SEM and gel electrophoresis. Reaction components were premixed in a 1.5-ml Eppendorf centrifuge tube with enough buffer (50 mM Tris-HCl, 100–150 mM NaCl, pH 7.5) to bring the total volume to 330 μl and maintain the final ionic strength at 0.15. After the addition of thrombin, the last step for initiating coagulation, the reaction components were thoroughly mixed with a pipette tip, and 325 μl of the clotting mixture were quickly transferred from the tube to the stainless steel rheometer cone and plate fixture (which had a 2.5° cone angle and 30 mm diameter). Measurements were taken at 0.1 Hz under an imposed strain of 0.015. For measuring purposes, the rheometer was operated in an oscillatory mode, with data collected over 10-s periods every 2 min. Between the 2-min intervals, the clot remained at rest. The storage modulus (G'), a measure of the elastic energy stored during the deformation imposed by one oscillation of the rheometer, was calculated by Bohlin VOR Rheometer Software Version 4.05 (Bohlin Reologi AB, Sweden) and used as a measure of clot rigidity. The loss modulus (G''), which reflects the energy dissipated by the clot during deformation, was also recorded and used to calculate the loss tangent ($\tan \delta = G''/G'$), the ratio of energy lost to energy stored in a cyclic deformation. Coagulation proceeded at 21°C. To prevent dehydration, heavy mineral oil (Walgreen Co., Deerfield, IL) was applied to a ring surrounding the exposed surfaces of the clots at the beginning of the experiments.

Measurement of clotting time

Reaction mixtures comprised of fibrinogen (3 mg/ml), thrombin (0.25, 0.5, 1 NIHU/ml) and FXIIIa inhibitor (L682777, 1 mM) were mixed at room temperature (20–22°C) in borosilicate culture tubes (12 × 75 mm, Baxter Healthcare Corp., McGaw Park, IL). Enough buffer (50 mM Tris-HCl, 100–150 mM NaCl, pH 7.5) was used to bring the volumes to 500 μl and maintain the final ionic strength at 0.15. After the addition of thrombin, the last step for initiating coagulation, the reaction components were gently swirled in the tube and tilted every 15 s until clot formation was visually detected. The times at which the clots were formed were recorded.

Samples having the same compositions as those formed in the tubes were analyzed by rheometry. The G' values established by the clots at their previously recorded times of appearance in the culture tubes were taken to be the rigidities of the clots developed at their initial formation. The average of these G' values was 0.73 ± 0.16 Pa. In subsequent rheometry experiments, clotting time was defined as the time at which sample rigidity reached 0.73 Pa.

Analysis of fibrin cross-linking by SDS-PAGE

Electrophoretic experiments to assess the cross-linking profiles of clots were carried out on mixtures of compositions identical to those used for rheological measurements and SEM analysis. Clots were formed at 21°C in 25 μl reaction mixtures. The ligating reaction in the samples was stopped by solubilization in 6 M urea, 40 mM dithiothreitol, and 2% SDS at 37°C for 45–60 min. Gel electrophoresis (8% acrylamide) was performed by the procedure of Laemmli (1970) in a Mini-Protean II Dual Slab Cell (BioRad, Hercules, CA). Samples of ~6 μg protein per lane were analyzed, and a broad-range molecular weight standard (BioRad) was used for reference. Coomassie brilliant blue R (0.025% in 10% acetic acid and 20% methanol) was used for staining. Photographs of the gels focus on the protein bands with M_r values higher than 31,000. Relative intensities of Coomassie blue-stained bands were measured in an LKB Ultroscan XL Laser Densitometer (Bromma, Sweden) and quantitated by excising and weighing the peak areas.

RESULTS

Clot architecture

The reference clotting mixture in this study was composed of fibrinogen (3 mg/ml), thrombin (1 NIHU/ml) and FXIIIa inhibitor (1 mM), Figure 2 shows the changes in clot architecture as fibrinogen (Fig. 2 *A*) and thrombin (Fig. 2 *B*) concentrations were varied and as $CaCl_2$ was included in the mixture (Fig. 2 *C*). The latter also shows the architecture of ligated clots formed by omitting the FXIIIa inhibitor and adding $CaCl_2$. Fig. 3 shows the quantitative results of analyses of these clots by computerized three-dimensional modeling. Fiber diameters decreased (from 72 to 46 nm) as the fibrinogen concentration increased from 0.5 to 6 mg/ml, decreased (108 to 44 nm) as the thrombin concentration increased from 0.05 to 5 NIHU/ml, and increased (85 to 147 nm for unligated and 69 to 131 nm for ligated) as the $CaCl_2$ concentration increased from 0.2 to 20 mM. Fiber lengths were relatively insensitive to fibrinogen concentration (range: 0.8–0.4 μm), decreased (4.0–0.3 μm) with increased thrombin concentration, and increased (1.0 to 3.9 μm for unligated and 1.1 to 4.8 μm for ligated) as the Ca^{2+} increased. Fiber and branchpoint densities were relatively insensitive to fibrinogen concentration between 0.5 and 3

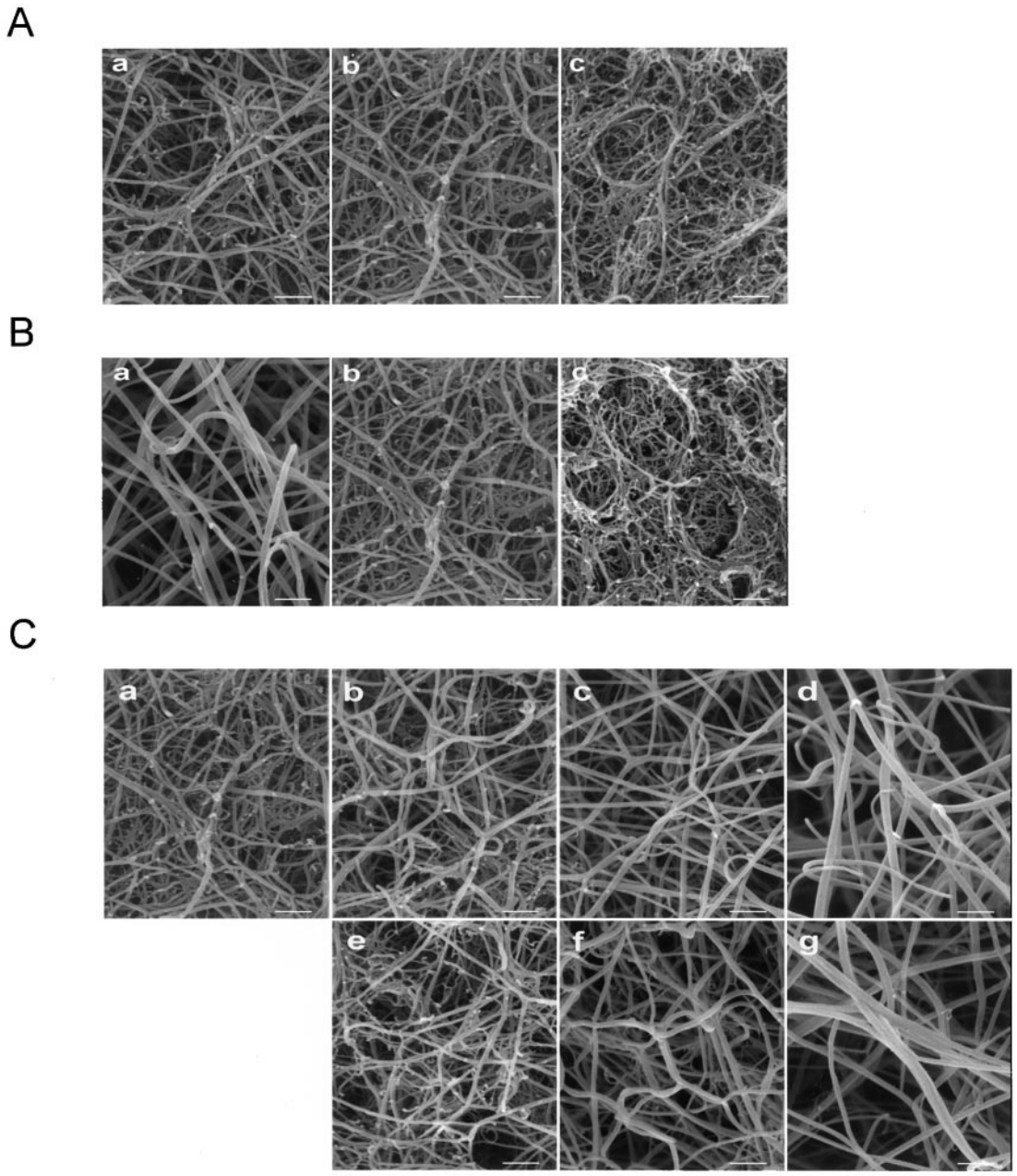

FIGURE 2 Scanning electron micrographs of clots formed with varying mixtures. (*A*) Reaction mixtures were comprised of fibrinogen [0.5 (*a*), 3 (*b*), or 6 (*c*) mg/ml], thrombin (1 NIHU/ml), and FXIIIa inhibitor (1 mM). (*B*) Reaction mixtures were comprised of fibrinogen (3 mg/ml), thrombin [0.05 (*a*), 1 (*b*), or 5 (*c*) NIHU/ml], and FXIIIa inhibitor (1 mM). (*C*) Reaction mixtures were comprised of fibrinogen (3 mg/ml), thrombin (1 NIHU/ml), $CaCl_2$ [0 (*a*), 0.2 (*b, e*), 5 (*c, f*), or 20 (*d, g*) mM], and 1 mM (*a–d*) or 0 mM (*e–g*) FXIIIa inhibitor. Clots were incubated for 2 h at 20–22°C. Bar = 0.5 μm.

mg/ml, but both increased over threefold at 6 mg/ml. Despite these changes at the high fibrinogen concentration, the lengths of the fibers remained relatively constant, indicating that the increased branchpoint density at the high fibrinogen concentration resulted from greater density of fiber structures and not from an increased incidence of branching along the fibers. The similarity between the fiber densities and diameters of samples formed from 0.5 and 3 mg/ml fibrinogen may be explained by the possible greater shrinkage of the clot volume at the lower concentration of the protein during critical point drying. Fiber and branchpoint densities increased manyfold with increased thrombin concentration, whereas they decreased manyfold with increased $CaCl_2$.

Figs. 2 *C* and 3 *C* also show comparisons between unligated and ligated clots with variations in $CaCl_2$ concentrations and suggest no major differences in lengths, diameters, or fiber and branchpoint densities between the two types of clots. Large-sample tests, however, reveal that the differences in fiber lengths (ligated clot fibers were 11 to 22% longer) and fiber diameters (ligated clot fibers were 11 to 19% smaller in diameter) were statistically significant, $p <$

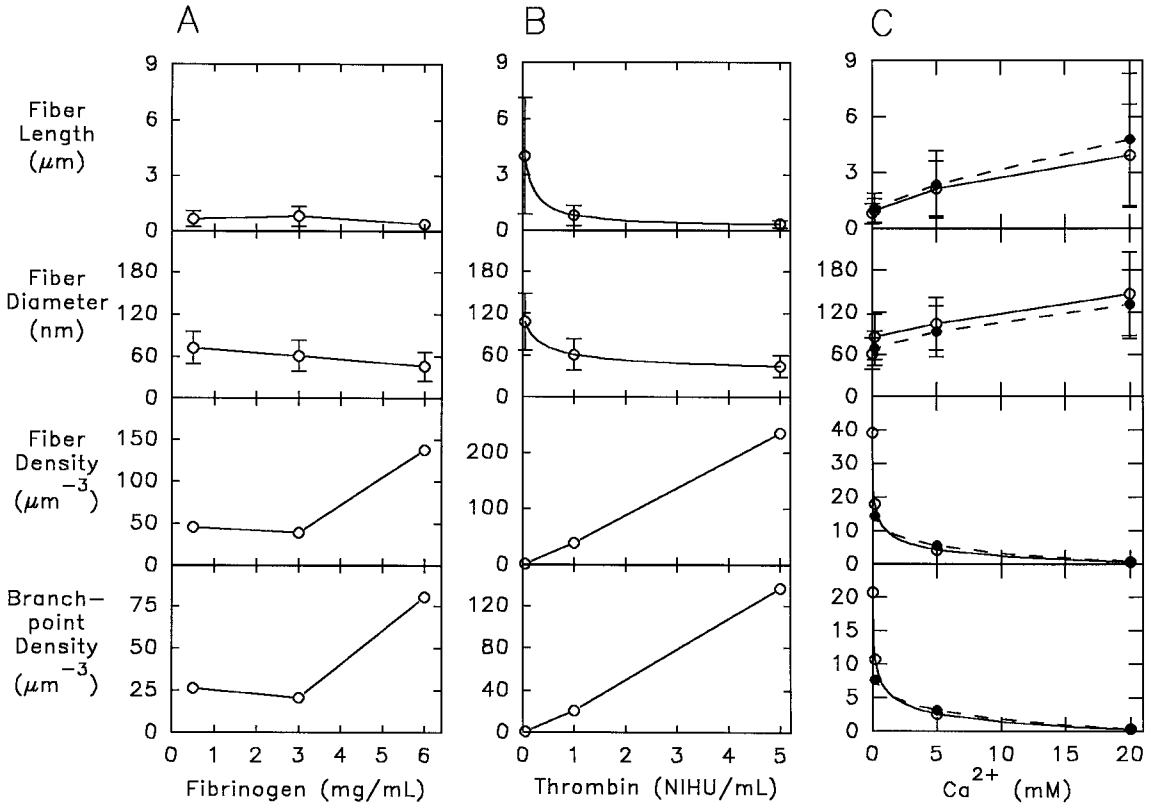

FIGURE 3 Effects of mixture constituents on the architecture of the fibrin networks shown in Fig. 2. (*A*) Effects of fibrinogen concentration on the unligated fibrin networks shown in Fig. 2 *A*. (*B*) Effects of thrombin concentration on the unligated fibrin networks shown in Fig. 2 *B*. (*C*) Effects of calcium concentration on the fibrin networks shown in Fig. 2 *C*. Clots were formed with 0 mM (*solid symbols*) or 1 mM (*open symbols*) FXIIIa inhibitor. Error bars represent standard deviations of the data.

0.0103 and $p < 0.000003$, respectively. These results suggest that the covalent bonds formed with the presence of FXIIIa significantly tightens the lateral attachments between fibrin molecules within a fiber, but does not add or subtract more fibrin monomers to each fiber. Tables 1 and 2 summarize the compositions and network characteristics for all the clots developed in this investigation.

Clot rheology

Figs. 4–6 shows the physical properties of clots (using the same mixtures as those formed for the SEM) as a function of the fibrinogen, thrombin, and $CaCl_2$ concentrations, respectively. A clotting period of 2 h was found to be sufficient to effect essentially full development of clot stiffness with all variations of fibrinogen concentration (Fig. 4). Final stiffnesses (G' at 2 h) were proportional to the 1.67 power of the starting fibrinogen (c) concentration, consistent with the results of Ferry and Morrison (1947); Roberts et al. (1974); Gerth et al. (1974); and Nelb et al. (1976), who reported the concentration dependence of G' for unligated fibrin clots to vary between $c^{1.5}$ and $c^{1.57}$. Other investigators reported relationships of $G' \sim c^2$ (fibrin clots formed with 0.05–0.8 mg/ml fibrinogen; Shen et al., 1975), $G' \sim c^{2.1}$ (fibrin clots formed with 5–20 mg/ml fibrinogen; Fukada and Kaibara, 1973); $G' \sim c^{1.7}$ (plasma clots, Fukada and Kaibara, 1973), and $G' \sim c$ (platelet free plasma clots; Glover et al., 1975). At 2 h, values of the loss modulus (G'') were ~20–40 times smaller than those of G', as reflected by the small values of the loss tangent ($\tan \delta = G''/G'$). The loss moduli at 2 h were proportional to the 1.44 power of fibrinogen concentration ($G'' \sim c^{1.44}$). The value of $\tan \delta$ for the sample containing no fibrinogen could not be accurately determined, due to the limited sensitivity of the rheometer in recording values of G' and G'' at very small substrate concentrations. As substrate concentrations were raised from 0.5 to 6 mg/ml, values of $\tan \delta$ decreased slightly.

TABLE 1 Compositions of clots analyzed

Clot	Fibrinogen (mg/ml)	Thrombin (NIHU/ml)	$CaCl_2$ (mM)	FXIIIa inhibitor (mM)
A	0.5	1	0	1
B	3	1	0	1
C	6	1	0	1
D	3	0.05	0	1
E	3	5	0	1
F	3	1	0.2	1
G	3	1	5	1
H	3	1	20	1
I	3	1	0.2	0
J	3	1	5	0
K	3	1	20	0

TABLE 2 Summary of quantitative measurements of fibrin network features

Clot*	Number of Fiber Lengths Measured	Estimated Fiber Length (μm) (Mean ± SD)	Range of Fiber Lengths (μm)	Number of Fiber Diameters Measured	Fiber Diameter (nm) (Mean ± SD)	Range of Fiber Diameters (nm)	Fiber Density (fibers, μm^{-3})	Branchpoint Density (branchpts, μm^{-3})
A	1104	0.7 ± 0.4	0.1–3.2	523	72 ± 23	28–201	42	26
B	985	0.8 ± 0.5	0.1–6.4	564	61 ± 22	17–196	35	21
C	909	0.4 ± 0.2	0.1–2.0	572	46 ± 21	16–183	125	80
D	516	4.0 ± 3.1	0.3–15	563	108 ± 40	26–325	1.2	0.8
E	977	0.3 ± 0.2	0.1–1.3	581	44 ± 15	20–130	215	137
F	760	1.0 ± 0.7	0.1–5.2	580	85 ± 32	28–285	17	11
G	750	2.1 ± 1.5	0.2–7.9	597	104 ± 37	33–313	3.8	2.6
H	620	3.9 ± 2.8	0.4–16	577	147 ± 59	41–391	0.5	0.4
I	924	1.1 ± 0.8	0.1–5.8	573	69 ± 24	27–226	13	7.7
J	521	2.4 ± 1.8	0.2–8.3	573	93 ± 36	27–281	4.8	3.2
K	635	4.8 ± 3.5	0.4–19	557	131 ± 49	41–352	0.6	0.4

*Refer to Table 1 for clot compositions.

Clotting times gradually increased as fibrinogen concentrations were raised.

A clotting period of 15 h was necessary to effect essentially full development of clot stiffness for some of the thrombin concentrations utilized (Fig. 5). With low thrombin concentrations (0.1 and 0.25 NIHU/ml) the rate of stiffness development is slow but the final stiffness is relatively high compared to those formed with more thrombin. Clotting times decreased dramatically between 0 and 1 NIHU/ml and appeared to approach their minimum levels above 1 NIHU/ml. Values of G' at 2 (*open circles*) and 15 h (*open triangles*) rose sharply between 0 and 0.25 NIHU/ml and then decreased to lower plateauing values as thrombin levels increased to 5 NIHU/ml. The G' values observed at 2 h at low thrombin concentrations (below 0.1 NIHU/ml) were small due to incomplete clot development. The rates of stiffening at these low enzyme concentrations were so diminished that, at time periods even longer than 2 h, "final" rigidities would still likely have been smaller than those of clots formed at concentrations near 0.1 NIHU/ml. A maximum rigidity at 2 h occurred at a thrombin concentration (0.25 NIHU/ml) that yielded a network with fiber lengths of ~2 μm, diameters of ~83 nm, fiber densities of ~9.3 μm^{-3}, and branchpoint densities of ~5 μm^{-3} (see Fig. 3

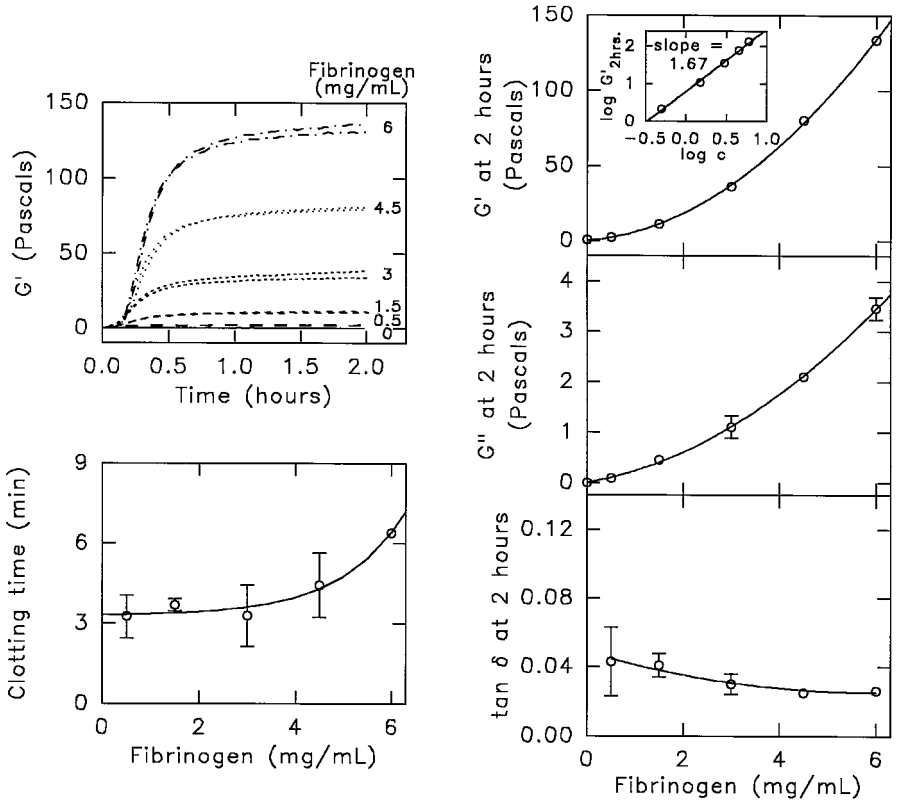

FIGURE 4 Clotting time and rheological behavior of unligated clots formed with varying concentrations of fibrinogen. Clots were formed at 21°C from solutions of fibrinogen (0, 0.5, 1.5, 3, 4.5, 6 mg/ml), thrombin (1 NIHU/ml), and FXIIIa inhibitor (1 mM). Clotting times and values of G', G'', and tan δ were averaged from two sets of data; error bars represent ranges of the data.

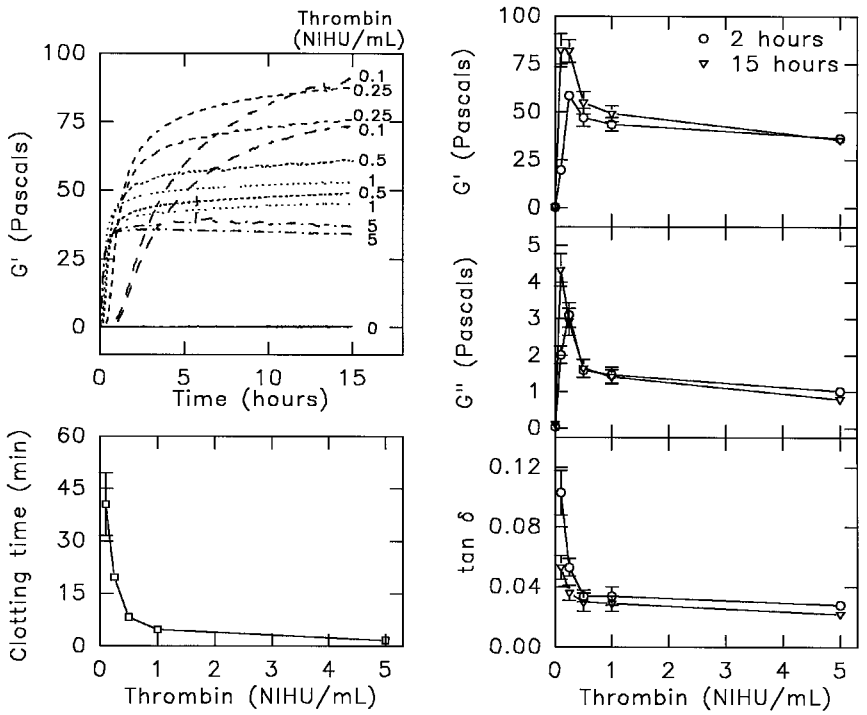

FIGURE 5 Clotting time and rheological behavior of unligated clots formed with varying concentrations of thrombin. Clots were formed at 21°C from solutions of fibrinogen (3 mg/ml), thrombin (0, 0.1, 0.25, 0.5, 1, 5 NIHU/ml), and FXIIIa inhibitor (1 mM). Clotting times and values of G', G'', and tan δ at 2 h (*open circles*) and 15 h (*open triangles*) were averaged from two sets of data; error bars represent ranges of the data.

B). These fiber sizes and fiber and branchpoint densities were "intermediate" in magnitude, relative to the entire range of fiber sizes and fiber and branchpoint densities measured in this investigation (see Table 2). The peaking behavior observed in G' at 2 and 15 h was also reproduced in G'' at 2 and 15 h, although values of the loss moduli were ~10–45 times smaller than those of the storage moduli. No clotting was observed in the absence of thrombin and the limited sensitivity of the rheometer prevented an accurate determination of the loss tangent for samples formed with 0 NIHU/ml thrombin. The tan δ, however, dropped sharply between 0.1 and 0.5 NIHU/ml thrombin and decreased to lower plateauing values between 0.5 and 5 NIHU/ml. A similar decrease in tan δ was observed by Kaibara and Fukada (1971) between 0.2 and 1.7 NIHU/ml thrombin.

Two hours were sufficient for essentially developing the full clot stiffness for all variations of $CaCl_2$ concentrations for unligated clots, but not sufficient for many $CaCl_2$ concentrations for ligated clots (Fig. 6). The 2-h G' values of clots formed with inhibitor (*open circles*) were two to four times smaller than those formed without inhibitor (*solid circles*). The G' values of clots measured at 2 h increased as calcium rose from 0 to 1.5 mM and then decreased at concentrations above 1.5 mM. The changes in clot stiffness were not due to differences in ionic strength, for the NaCl concentrations in the buffer solution were adjusted to maintain a constant ionic strength in all the samples. Consistent with the results of the experiment in which thrombin concentrations were varied, the maximum rigidities for samples formed both in the presence and absence of inhibitor occurred at a calcium ion concentration (1.5 mM, the normal physiological level in plasma) that produced a network structure with fiber lengths (~1.3 μm, unligated; ~1.4 μm, ligated), diameters (~90 nm, unligated; ~75 nm, ligated), densities (~8.4 μm^{-3}, unligated; ~9.1 μm^{-3}, ligated), and degrees of branching (~5.1 μm^{-3}, unligated and ligated) that were "intermediate" (see Fig. 3 *C*). The loss moduli of the samples formed without inhibitor were two to four times smaller than those formed with inhibitor. At 2 h, the values of G'' were ~60–230 times smaller than G' for the ligated clots and ~10–20 times smaller for the unligated clots. The loss tangent for both clot types steadily increased as calcium concentrations were raised from 0 to 5 mM and increased at much slower rates from 5 to 20 mM $CaCl_2$. Clotting times decreased sharply as calcium concentrations were raised from 0 to 2.5 mM and then plateaued to constant minimums between 5 and 20 mM. The rates of clotting for both the ligated and unligated samples were similar at all calcium ion concentrations.

Cross-link analysis

Fig. 7 shows the cross-link analysis by SDS-PAGE for clots having compositions equal to those formed for the SEM and clot rheology. It reveals that in the presence of 1 mM inhibitor no ligating of the fibrin γ- or α-chains occurred within the range of calcium concentrations used (Fig. 7 *A*). In the absence of FXIIIa inhibitor, full depletion of γ monomers and formation of γ-dimers occurred by 0.2 mM $CaCl_2$ (Fig. 7 *B*). A progressive depletion of the α-monomers occurred as $CaCl_2$ was raised from 0.2 to 20 mM, resulting in the formation of bands that have customarily been identified as α_n-polymers and ligated αγ-hybrids. Fig.

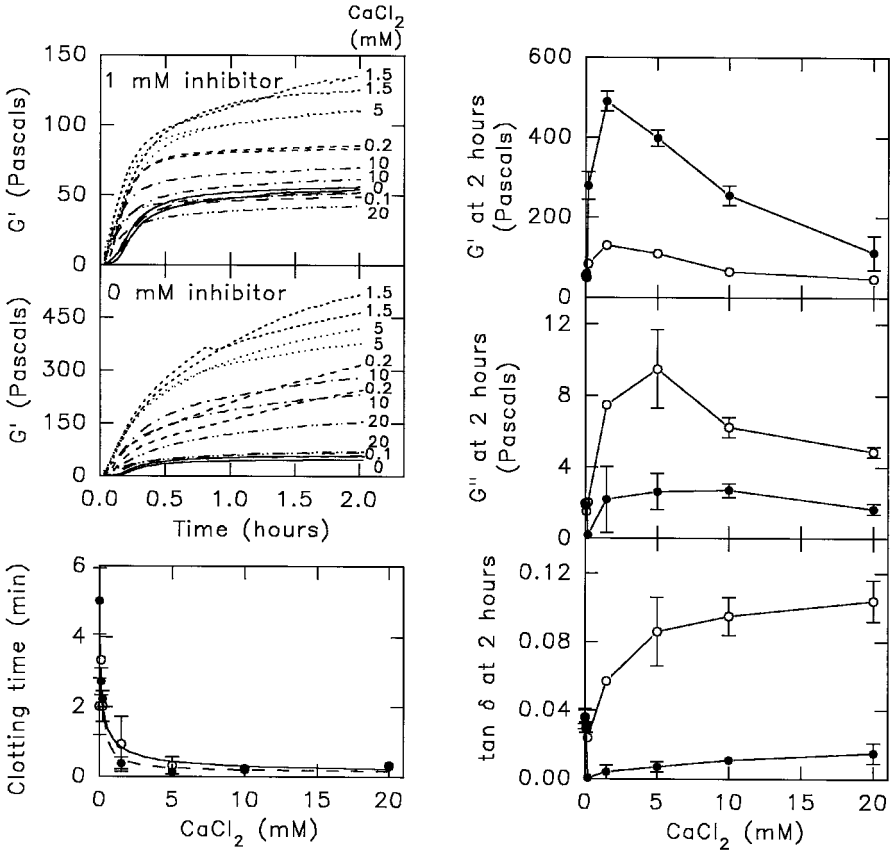

FIGURE 6 Clotting time and rheological behavior of clots formed with varying concentrations of calcium. Clots were formed at 21°C from solutions of fibrinogen (3 mg/ml), thrombin (1 NIHU/ml), $CaCl_2$ (0, 0.1, 0.2, 1.5, 5, 10, 20 mM), and 0 mM (*solid symbols*) or 1 mM (*open symbols*) FXIIIa inhibitor. Clotting times and values of G', G'', and tan δ were averaged from two sets of data; error bars represent ranges of the data.

6 shows that clots formed without inhibitor continued to stiffen past 2 h, particularly at intermediate calcium concentrations (0.2–5 mM), at which time full depletion of the α-chains by ligating had not occurred (see Fig. 7 *B*).

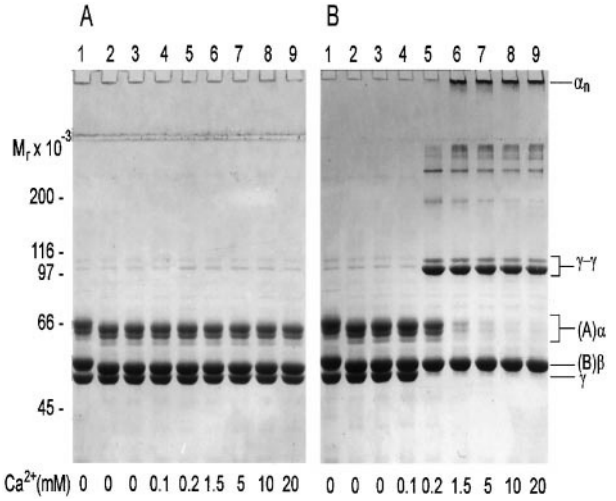

FIGURE 7 Reducing SDS-PAGE analysis of cross-linked chain profiles at varying concentrations of calcium ion. Reaction mixtures (all containing 3 mg/ml fibrinogen) were clotted at 21°C for 2 h with EDTA (1 mM), *lane 1*; thrombin (1 NIHU/ml) and EDTA, *lane 2*; and thrombin and $CaCl_2$ (0–20 mM) *lanes 3–9*. Samples included 1 mM (*A*) or 0 mM (*B*) FXIIIa inhibitor.

Characteristic features of fibrin network formation

Close examination of the fiber characteristics observed under all the clotting conditions revealed definite patterns in the manner in which normal fibrin assembles. Fiber densities were consistently ~1.56 times greater than their branchpoint densities (Fig. 8). Large fiber diameters and lengths were established only when branching was minimal, and increases in fiber lengths generally appeared to be accompanied by increases in fiber diameters (Fig. 9).

Fiber lengths and diameters decreased with increased branching but did not further decrease above branchpoint densities of 25 μm^{-3} (Fig. 8). Above this level, fibers appeared to have reached their minimum sizes. Fiber lengths plateaued to an average minimum length of 463 nm, and fiber diameters decreased to an average minimum of 54 nm [~10 monomers long and ~6–9 monomers thick, based on the 45-nm length and 6–9-nm width of a fibrinogen molecule measured by Hall and Slayter, 1959; Bachmann et al., 1975; and Estis and Haschemeyer, 1980].

DISCUSSION

Determinants of clot structure

The kinetics of fibrin polymerization govern the structure of a fibrin network (Hantgan and Hermans, 1979; Wolfe and

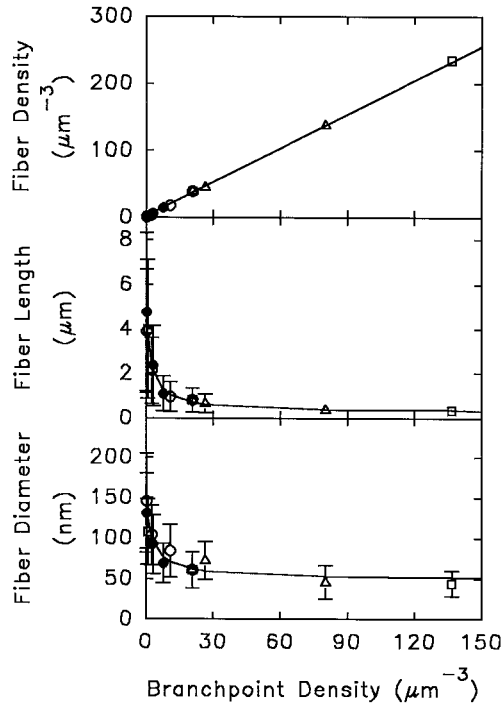

FIGURE 8 Effect of branchpoint density on fiber density, fiber length, and fiber diameter. Data were obtained from the experiments in which fibrinogen concentration was varied (Fig. 3 *A, open triangles*), thrombin concentration was varied (Fig. 3 *B, open squares*), and calcium ion concentration was varied (Fig. 3 *C, open circles*, unligated; *solid circles*, ligated). Error bars represent standard deviations of the data.

Waugh, 1981; Blomback and Okada, 1982; Shah et al., 1985; Carr et al., 1986; Weisel and Nagaswami, 1992). The influence of the rates of polymerization on clot architecture is clearly demonstrated in the modulation of fiber sizes by varying concentrations of thrombin (Figs. 2 *B* and 3 *B*). The observed effect of higher thrombin concentrations on diminishing fiber size is consistent with the results of permeability experiments (Blomback et al., 1990), turbidity experiments (Shah et al., 1985; Carr, 1988; and Blomback et al., 1990), and electron microscopy (Weisel and Nagaswami, 1992). Lowering the concentration of the enzyme reduces the rate of fibrinopeptide cleavage, resulting in a slower production of fibrin monomers. Existing protofibrils grow longer and aggregate laterally as monomers are slowly produced, resulting in a network of long, thick fibers (Weisel and Nagaswami, 1992). At higher thrombin concentrations, the rate of lateral and lengthwise fiber growth is slow compared to the rate of fibrinopeptide cleavage. Thus, several short oligomers are formed before they can join lengthwise or associate laterally, resulting in a network of thin, short fibers.

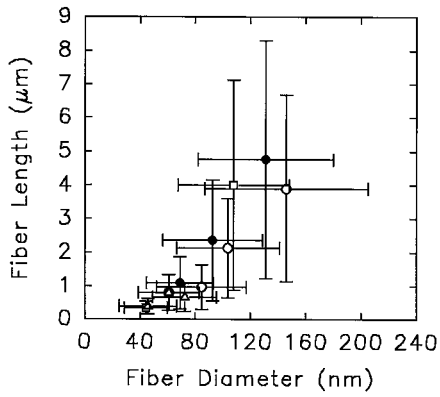

FIGURE 9 Dependence of fiber length on fiber diameter. Data were obtained from the experiments in which fibrinogen concentration was varied (Fig. 3 *A, open triangles*), thrombin concentration was varied (Fig. 3 *B, open squares*), and calcium ion concentration was varied (Fig. 3 *C, open circles*, unligated; *solid circles*, ligated). Error bars represent standard deviations of the data.

Similar effects of decreased fiber size are observed as fibrinogen concentrations are increased (Figs. 2 *A* and 3 *A*). Raising the concentration of fibrinogen might be expected to lead to thicker fibers because of the decreased thrombin-to-fibrinogen ratios (Weisel and Nagaswami, 1992), as reflected in the longer clotting times. However, the decreased fiber diameters may be attributed to accelerated rates of monomer formation because of higher substrate concentrations. Similar decreases in fiber mass-to-length ratio were observed in turbidity experiments on plasma clots by Carr and Carr (1995), in permeability studies on fibrin clots by Rosser et al. (1977), and in recent electron microscopy experiments (Herbert et al., 1998). Other investigators, however, reported increases (Shah et al., 1985) or no changes (Blomback et al., 1990) in fiber mass-to-length ratio with increases in fibrinogen. Further studies maintaining constant ratios of thrombin to fibrinogen would be useful in resolving the effects of fibrinogen concentration on clot organization.

The increased fiber sizes in clots formed at elevated calcium concentrations (Figs. 2 *C* and 3 *C*) are consistent with the results of turbidity experiments by Okada and Blomback (1983), Carr (1988), and Carr and Carr (1995). Calcium has long been known to have an accelerating effect on fibrin clotting (Rosenfeld and Janszky, 1952; Ratnoff and Potts, 1954), due to the enhancement of one or more polymerization events subsequent to fibrinopeptide cleavage (Lorand and Konishi, 1964; Boyer et al., 1972; Endres and Scheraga, 1972; Brass et al., 1978; Blomback et al., 1978; Hardy et al., 1983). Dang et al. (1989) suggested that lateral aggregation is enhanced through decreases in charge from the binding of calcium to sialic acid on the carbohydrates of fibrinogen. Increased calcium binding to fibrin during polymerization also has been correlated with the removal of fibrinopeptide B (Mihalyi, 1988). Calcium enhances the affinity of GHRP (the N-terminal tetrapeptide of the fibrin β-chain exposed after fibrinopeptide B release) for fibrinogen (Laudano and Doolittle, 1981), thereby stabilizing the protofibril and promoting its lengthwise growth and lateral aggregation (Hantgan and Hermans, 1979; Hantgan et al., 1980, 1983; Fowler et al., 1981).

The modulation of clot structure caused by changing the rates of one or more steps of polymerization largely explains the characteristic networks observed in this investigation. Under conditions that promote the formation of long protofibrils, lateral aggregation is favored. Long fiber lengths are, therefore, generally accompanied by large fiber diameters (Fig. 9), as described by Baradet et al. (1995). Branching becomes less frequent under conditions that promote lengthwise protofibril growth. The divergence of protofibrils from parent fibers may be inhibited by the increased strength of binding acquired through the cumulation of weak noncovalent interactions along the long protofibrils. Small branchpoint densities are, therefore, observed in networks that have great fiber lengths and diameters (Fig. 8).

A strong correlation between fiber density and branchpoint density was recognized in all the networks examined (Fig. 8). The ratio of fiber density to branchpoint density remained near 1.56 in every case (1.56 ± 0.07), indicating that an optimal degree of branching existed, regardless of fiber size or the conditions under which the networks were formed. During the construction of the computerized three-dimensional fibrin network models, three or, occasionally, four fibers were observed to join at a branchpoint. In rare instances, more than four fibers at a branchpoint were seen. These latter observations, however, were usually made at locations at which the ability to distinguish the arrangement of several coalescing fibers was limited by the resolution of the micrographs. To characterize the branching observed in the clots, the fiber-to-branchpoint ratios for models of "perfect" polymeric networks having constant degrees of branching were calculated using the equation $\nu/\mu = \phi/2$ (Flory, 1953; Mark, 1982), in which ν = number of network fibers, μ = number of network junctions, and ϕ = number of chains meeting at each junction. Molecular theories describing polymeric networks define "perfect" networks to be those that have no dangling fibers (fibers connected to a junction of the network at only one end) or loops (fibers having both ends attached to the same junction). Although these types of networks do not occur in reality, the fibrin clots examined displayed no loops and few fibers with naturally occurring dangling ends. From the above equation, a perfect network with three fibers joining at every junction has a fiber-to-branchpoint ratio of 1.5. The ratio increases to 2 for networks in which four fibers join at each junction and continues to rise as the degree of branching increases. Based on these models, the experimentally determined fiber-to-branchpoint ratio of 1.56 indicates that junctions at which three fibers join are the dominant branchpoint type. In their quantitative study of clot structure, Baradet et al. (1995) also described a dominant number (three) of branchpoints at every junction. Mosesson et al. (1993) described two types of branching junctions in fibrin fibers formed in vitro, but either type of junction would produce branchpoints at which three fibers join.

Effects of network structure on clot rigidity

Pronounced increases in clot rigidity (G') were obtained as fibrinogen concentrations were raised (Fig. 4). The increased incidence of myocardial infarction in patients with elevated levels of plasma fibrinogen has been attributed, in part, to the less deformable clots formed at these concentrations (Scrutton et al., 1994), but the densely packed structures observed at higher substrate levels may also contribute to limited fibrinolysis. The small degree of change in fiber diameters and lengths exhibited in this fibrinogen range indicates that the most probable cause for the bolstered clot rigidity at higher substrate levels is not the changes in fiber structure, but rather the increased density of fibers resulting from the greater total mass of protein.

In contrast, modifications of fiber structure were most likely responsible for the variances in rigidity observed in clots formed with changing thrombin and calcium levels. The peaking behavior of final clot rigidity with increasing calcium concentration is consistent with the findings of Shen et al. (1974, 1975); Marx (1988); Caprini et al. (1974); and Carr and Carr (1995). The observed increase of final clot stiffness between 0 and 0.25 NIHU/ml thrombin has also been demonstrated by other investigators (Kaibara and Fukada, 1971; Kaibara, 1973; Marx, 1988), but the detection of clot softening at higher levels of thrombin is unique to this investigation. The observed clot softening is not likely to be due to the digestion of fibrin by thrombin (Triantaphyllopoulos and Chandra, 1973; Kang and Triantaphyllopoulos, 1977a, b), as evidenced by the absence of digested fibrin chain products in samples analyzed by reducing SDS-PAGE after 2 h of clotting with 0 to 1 NIHU/ml thrombin (data not shown). Although a small percentage of α-chain digestion was detected at 5 NIHU/ml thrombin, 68% of the decrease in clot rigidity had already been established between 0.25 and 1 NIHU/ml. The fiber lengths, diameters, and fiber and branchpoint densities that generated maximum rigidities in the thrombin experiments were strikingly similar to those producing peak stiffnesses in the calcium experiments. The maximally stiff networks of the thrombin and calcium experiments exhibited fiber lengths of ~2 and ~1.3–1.4 μm, fiber diameters of ~83 and ~75–90 nm, fiber densities of ~9.3 and ~8.4–9.1 μm^{-3}, and branchpoint densities of ~5 and ~5.1 μm^{-3}, respectively.

Our results suggest that network stiffness is strongly dependent on fiber thickness and branchpoint concentration. The greater branching observed at high thrombin or low calcium concentrations contributes to increased clot rigidity; however, the reduction of fiber diameters accompanying increased branching softens the network. Clots exhibiting a balance between high branching density and large fiber diameters, therefore, manifest the greatest stiffness. This balance appears to occur in networks that display fiber sizes and branchpoint densities that are intermediate.

Although clots exhibiting these intermediate fiber characteristics are maximally rigid, their structures indicate that

they may not necessarily be maximally resistant to fibrinolysis. Gabriel et al. (1992) and Carr and Alving (1995) demonstrated that thinner fibers lyse at slower rates than thicker ones, although Kolev et al. (1997) obtained conflicting results. The softer clots formed with low calcium levels or high thrombin levels may be less susceptible to fibrinolysis. The peak stiffnesses generated with physiological levels of calcium (1.5–2 mM) may function to effectively arrest bleeding, yet the intermediate fiber sizes and densities established at these rigidities may give the clot the structure necessary for maintaining a proper balance between coagulation and fibrinolysis. Although normal plasma levels of prothrombin have been determined, 1 to 2 μM (Fenton et al., 1977) plasma concentrations of thrombin are suspected to vary considerably (Blomback et al., 1984), particularly at sites of lesions. The physiological significance of maximum rigidities developing with 0.25 NIHU/ml thrombin is, therefore, difficult to ascertain.

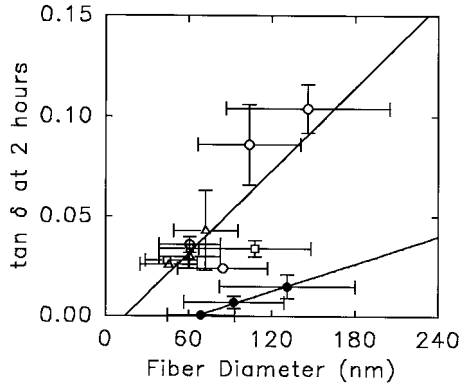

FIGURE 10 Dependence of loss tangent on fiber diameter. Data were obtained from the experiments in which fibrinogen concentration was varied (Fig. 3 *A, open triangles*), thrombin concentration was varied (Fig. 3 *B, open squares*), and calcium ion concentration was varied (Fig. 3 *C, open circles*, unligated; *solid circles*, ligated). Error bars represent standard deviations of the data.

Effects of network structure on energy dissipation during clot deformation

On a molecular basis, the dissipation of energy reflected by the loss modulus is believed to originate from molecular or atomic adjustments (Ferry, 1970). In a clot, these adjustments may arise from the dissociation of non-covalently linked adjacent fibrin monomers and the slippage of protofibrils or fibers between one another. In all of the experiments performed, the concentration dependence of G'' at 2 h closely mimicked that of G' at 2 h. A parameter that revealed more information about network structural rearrangements than G'' was the loss tangent, which reflects the ratio of energy dissipated to energy stored in a sample during deformation.

The network feature that showed the greatest effect on the loss tangent was fiber diameter. In all of the cases examined, smaller values of tan δ were produced in networks displaying smaller fiber diameters (Fig. 10), indicating that structural rearrangements between fibers or protofibrils were less common in clots having thinner fibers. The greater degree of branching observed in networks with thin fibers (see Fig. 8) may point to the importance of branching in inhibiting configurational rearrangements that result in the loss of elastic energy. At all fiber diameters, values of tan δ and G'' for the ligated networks were smaller than those of the unligated clots (Figs. 6 and 10). The presence of covalent linkages between the assembled fibrin monomers is believed to secure protofibrils together and prevent dissociations between adjacent molecules, resulting in reinforced networks that dissipate diminished levels of energy during deformation.

Effects of cross-linking on network structure

At all the calcium ion concentrations examined, the presence of ligations was shown to slightly decrease network fiber diameters, causing concomitant increases in their lengths (Fig. 3 *C*). This effect was observed even at 0.2 mM $CaCl_2$, at which γ-chain ligating is complete by 2 h and α-chain ligating is just beginning (Fig. 7). The structural changes are not greatly enhanced as α-chain ligating is promoted at higher $CaCl_2$ concentrations, indicating that the altered fiber lengths and diameters may be caused by the formation of γ-chain cross-links alone.

The changes in fiber structure generated by ligating are small, relative to the entire range of structural changes observed in this investigation; qualitative differences between the morphology of the unligated and ligated networks are difficult to detect visually without the aid of direct measurements. Muller et al. (1984) reported no changes in the general appearance under electron microscopy of fibrin networks stabilized by FXIIIa, and the mass-length ratios of fibers examined in turbidity experiments (Carr et al., 1987) were not affected by FXIIIa-induced stabilization, although fiber densities did increase. The changes in fiber length and diameter brought about by ligating are most likely too small to solely account for the 2- to 4-fold augmentation of rigidity observed upon the introduction of ligations. Only minimal differences in fiber and branchpoint densities were detected between clots formed with and without FXIIIa inhibitor, indicating that the FXIIIa-induced enhancement of clot rigidity does not originate from alterations in network morphology (i.e., the formation of new branchpoints or increased lateral aggregation), but most likely from the stiffening of the individual fibers already existing. The tightening of lateral bonds between the fibrin monomers in a fiber brought about by the ligations could account for the slight decrease in fiber diameter, stiffening of the fibers, and the large increase in clot stiffness.

Evidence exists to suggest that the degree of stiffening produced by ligating may be dependent on network structure. The rigidity of a network having thick, long fibers and little branching is augmented 2.4 times when ligated in the

presence of 20 mM $CaCl_2$ (Fig. 6). At this calcium concentration, ligating causes a complete depletion of the α-chains (Fig. 7). A network with reduced fiber diameters but greater branching, however, requires a smaller percentage (68%) of the α-chains to be ligated for a greater (3.7-fold) enhancement of stiffness to be produced (at 1.5 mM $CaCl_2$). These results indicate that the augmentation of rigidity by ligating may be favored in networks that exhibit specific morphological features. For example, Mosesson et al. (1989) postulated that γ-trimers and γ-tetramers arise specifically at fibril branchpoints or at sites of lateral fiber association. In addition, γ-chain ligation has been shown to be favored under fine clotting conditions, whereas both α- and γ-chain ligations form under coarse conditions (Gerth et al., 1974). Elucidating the configuration of the various ligated species within the fibrin networks would be critical for determining their rheological effects on networks of varying structure. The possibility of regulating cross-link formation through the manipulation of network architecture remains to be explored.

CONCLUSIONS

The results of these experiments show that clot rheological behavior is regulated by at least the following three factors. *Fibrinogen concentration*: Increased fibrinogen concentrations elevate clot rigidities through the establishment of greater fiber and branchpoint densities. *Fibrin network architecture*: Fibrin polymerizes in a characteristic manner, allowing fibers to grow to sizable lengths and diameters only when branching is minimal. Maximal stiffnesses are manifested in clots that display fiber lengths, diameters, densities, and branchpoint densities that are intermediate in magnitude within the ranges observed. The high rigidities exhibited by clots that display this type of network morphology appear to result from a balance between a high degree of branching and thicker fibers, characteristics that both enhance network rigidity but are antithetical, since more branching leads to thinner fibers and thicker fibers yield less branching. Rearrangements in clot structure that lead to losses of elastic energy during deformation appear to be more common in clots having thicker fibers. *FXIIIa-induced ligation*: Ligating produces slight decreases in fiber diameter and increases in fiber length, but does not alter lateral aggregation or branching. Ligating appears to enhance clot rigidity and decrease clot loss modulus by stabilizing the interactions between preassembled protofibrils, thereby increasing fiber flexural stiffness. The degree to which the presence of ligations augments network rigidity appears to be dependent on the structure of the fibers stiffened.

We thank Lou Fodor for writing the image analysis software, with support from Dr. Lee Peachey under grant RR-2483 from the National Institutes of Health. We are also grateful to Dr. Wesley Burghardt for technical consultation and access to the rheometer, Dr. Takeru Igusa for aid with the censored data analysis, Dr. Andrew M. Stern for the inhibitor to FXIIIa, and Chandrasekaran Nagaswami for technical assistance and Dr. J. D. Ferry for helpful comments.

This work was supported by grants HL-02212 and HL-30954 from the National Institutes of Health.

REFERENCES

Bachmann, L., W. W. Schmitt-Fumian, R. Hammel, and K. Lederer. 1975. Size and shape of fibrinogen. 1. Electron microscopy of the hydrated molecule. *Makromol. Chem.* 176:2603–2618.

Baradet, T. C., J. C. Haselgrove, and J. W. Weisel. 1995. Three-dimensional reconstruction of fibrin clot networks from stereoscopic intermediate voltage electron microscope images and analysis of branching. *Biophys. J.* 68:1551–1560.

Blomback, B., D. Banerjee, K. Carlsson, A. Hamsten, B. Hessel, R. Procyk, A. Silveira, and L. Zacharski. 1990. Native fibrin gel networks and factors influencing their formation in health and disease. *In* Fibrinogen, Thrombosis, Coagulation and Fibrinolysis. C. Y. Liu and S. Chien, editors. Plenum Press, New York. 1–23.

Blomback, B., B. Hessel, D. Hogg, and L. Therkildsen. 1978. A two-step fibrinogen-fibrin transition in blood coagulation. *Nature (Lond.).* 275: 501–505.

Blomback, B., and M. Okada. 1982. Fibrin gel structure and clotting time. *Thromb. Haemostasis.* 25:51–70.

Blomback, B., M. Okada, B. Forslind, and U. Larsson. 1984. Fibrin gels as biological filters and interfaces. *Biorheology.* 21:93–104.

Boyer, M. H., J. R. Shainoff, and O. D. Ratnoff. 1972. Acceleration of fibrin polymerization by calcium ions. *Blood.* 39:382–387.

Brass, E. P., W. B. Forman, R. V. Edwards, and O. Lindan. 1978. Fibrin formation: effect of calcium ions. *Blood.* 52:654–658.

Caprini, J. A., H. C. Kwaan, L. Zuckerman, and R. Verduin. 1974. Thrombelastographic patterns of ancrod and thrombin fibrin formation and dissolution. *Thromb. Res.* 4:199–217.

Carr, M. E. 1988. Fibrin formed in plasma is composed of fibers more massive than those formed from purified fibrinogen. *Thromb. Haemostasis.* 59:535–539.

Carr, M. E., and B. M. Alving. 1995. Effect of fibrin structure on plasmin-mediated dissolution of plasma clots. *Blood Coagul. Fibrinolysis.* 6:567–573.

Carr, M. E., and S. L. Carr. 1995. Fibrin structure and concentration alter clot elastic modulus but do not alter platelet mediated force development. *Blood Coagul. Fibrinolysis.* 6:79–86.

Carr, M. E., D. A. Gabriel, and J. McDonagh. 1986. Influence of Ca^{2+} on the structure of reptilase-derived and thrombin-derived fibrin gels. *Biochem. J.* 239:513–516.

Carr, M. E., D. A. Gabriel, and J. McDonagh. 1987. Influence of factor XIII and fibronectin on fiber size and density in thrombin-induced fibrin gels. *J. Lab. Clin. Med.* 110:747–752.

Carr, M. E., and J. Hermans. 1978. Size and density of fibrin fibers from turbidity. *Macromolecules*. 11:46–50.

Carr, M. E., L. L. Shen, and J. Hermans. 1977. Mass-length ratio of fibrin fibers from gel permeation and light scattering. *Biopolymers.* 16:1–15.

Chen, R., and R. F. Doolittle. 1969. Identification of the polypeptide chains involved in the cross-linking of fibrin. *Proc. Natl. Acad. Sci. USA.* 63:420–427.

Chen, R., and R. F. Doolittle. 1971. γ–γ Cross-linking sites in human and bovine fibrin. *Biochemistry.* 10:4486–4491.

Dang, C. V., C. K. Shin, W. R. Bell, C. Nagaswami, and J. W. Weisel. 1989. Fibrinogen sialic acid residues are low affinity calcium binding sites that influence fibrin assembly. *J. Biol. Chem.* 264:15104–15108.

Doi, M., and N. Y. Kuzuu. 1980. Nonlinear elasticity of rodlike macromolecules in condensed state. *J. Polym. Sci., Polym. Phys. Ed.* 18: 409–419.

Doolittle, R. F., R. Chen, and F. Lau. 1971. Hybrid fibrin: proof of the intermolecular nature of γ–γ cross-linking units. *Biochem. Biophys. Res. Commun.* 44:94–100.

Endres, G. F., and H. A. Scheraga. 1972. Equilibria in the fibrinogen-fibrin conversion. IX. Effects of calcium ions on the reversible polymerization of fibrin monomer. *Arch. Biochem. Biophys.* 153:266–278.

Erickson, H. P., and W. E. Fowler. 1983. Electron microscopy of fibrinogen, its plasmic fragments and small polymers. *Ann. NY Acad. Sci.* 408:146–163.

Estis, L. F., and R. H. Haschemeyer. 1980. Electron microscopy of negatively stained and unstained fibrinogen. *Proc. Natl. Acad. Sci. USA.* 77:3139–3143.

Fenton, J. W., II, B. H. Landis, D. A. Walz, and J. S. Finlayson. 1977. Human thrombins. *In* Chemistry and Biology of Thrombin. R. L. Lundblad, J. W. Fenton, II, and K. G. Mann, editors. Ann Arbor Science, Ann Arbor, Michigan. 43–70.

Ferry, J. D. 1970. Viscoelastic Properties of Polymers. John Wiley and Sons, Inc., New York.

Ferry, J. D., M. Miller, and S. Shulman. 1951. The conversion of fibrinogen to fibrin. VII. Rigidity and stress relaxation of fibrin clots; effects of calcium. *Arch. Biochem. Biophys.* 34:424–436.

Ferry, J. D., and P. R. Morrison. 1947. Preparation and properties of serum and plasma proteins. IX. Human fibrin in the form of an elastic film. *J. Am. Chem. Soc.* 69:400–409.

Flory, P. J. 1953. Principles of Polymer Chemistry. Cornell University Press, Ithaca, New York.

Fowler, W. E., R. R. Hantgan, J. Hermans, and H. P. Erickson. 1981. Structure of the fibrin protofibril. *Proc. Natl. Acad. Sci. USA*. 78: 4872–76.

Freund, K. F., K. P. Doshi, S. L. Gaul, D. A. Claremon, D. C. Remy, J. J. Baldwin, S. M. Pitzenberger, and A. M. Stern. 1994. Transglutaminase inhibition by 2-[(2-oxopropyl)thio]imidazolium derivatives: mechanism of factor XIIIa inactivation. *Biochemistry.* 33:10109–10119.

Fukada, E., and M. Kaibara. 1973. The dynamic rigidity of fibrin gels. *Biorheology.* 10:129–138.

Gabriel, D. A., K. Muga, and E. M. Boothroyd. 1992. The effect of fibrin structure on fibrinolysis. *J. Biol. Chem.* 267:24259–24263.

Gerth, C., W. W. Roberts, and J. D. Ferry. 1974. Rheology of fibrin clots. II. Linear viscoelastic behavior in shear creep. *Biophys. Chem.* 2:208–217.

Gladner, J. A., and R. Nossal. 1983. Effects of cross-linking on the rigidity and proteolytic susceptibility of human fibrin clots. *Thromb. Res.* 30: 273–288.

Glover, C. J., L. V. McIntire, C. H. Brown, and E. A. Natelson. 1975. Rheological properties of fibrin clots. Effects of fibrinogen concentration, factor XIII deficiency, and factor XIII inhibition. *J. Lab. Clin. Med.* 86:644–656.

Glover, C. J., L. V. McIntire, C. H. Brown, and E. A. Natelson. 1977. Mechanical trauma effect on clot structure formation. *Thromb. Res.* 10:11–25.

Gorkun, O. V., Y. I. Vecklich, L. V. Medved, A. H. Henschen, and J. W. Weisel. 1994. Role of the αC domains of fibrin in clot formation. *Biochemistry.* 33:6986–6997.

Gron, B., C. Filion-Myklebust, A. Bennick, W. Nieuwenhuizen, G. R. Matsueda, and F. Brosstad. 1992. Early cross-linked fibrin in human plasma contains α-polymers with intact fibrinopeptide A. *Blood Coagul. Fibrinolysis.* 3:731–736.

Gron, B., C. Filion-Myklebust, S. Bjornsen, P. Haidaris, and F. Brosstad. 1993. Cross-linked $\alpha_s\gamma_t$-chain hybrids in plasma clots studied in 1D and 2D electrophoresis and Western blotting. *Thromb. Haemostasis.* 70: 438–422.

Hall, C. E., and H. S. Slayter. 1959. The fibrinogen molecule: its size, shape, and mode of polymerization. *J. Biophys. Biochem. Cytol.* 5:11–17.

Hantgan, R. R., W. Fowler, H. Erickson, and J. Hermans. 1980. Fibrin assembly: a comparison of electron microscopic and light scattering results. *Thromb. Haemostasis.* 44:119–124.

Hantgan, R. R., and J. Hermans. 1979. Assembly of fibrin. *J. Biol. Chem.* 254:11272–11281.

Hantgan, R. R., J. McDonagh, and J. Hermans. 1983. Fibrin assembly. *Ann. NY Acad. Sci.* 408:344–366.

Hardy, J. J., N. A. Carrell, and J. McDonagh. 1983. Calcium ion functions in fibrinogen conversion to fibrin. *Ann. NY Acad. Sci.* 408:279–287.

Herbert, C. B., C. Nagaswami, G. D. Bittner, J. A. Hubbell, and J. W. Weisel. 1998. Effects of fibrin micromorphology and density on neurite growth from dorsal root ganglia cultured within three-dimensional fibrin gels. *J. Biomed. Mater. Res.* 40:551–559.

Janmey, P. A., E. J. Amis, and J. D. Ferry. 1983. Rheology of fibrin clots. VI. Stress relaxation, creep, and differential dynamic modulus of fine clots in large shearing deformations. *J. Rheol.* 27:135–153.

Kaibara, M. 1973. Dynamic viscoelastic study of the formation of fibrin networks in fibrinogen-thrombin systems and plasma. *Biorheology.* 10: 61–73.

Kaibara, M., and E. Fukada. 1970. Dynamic viscoelastic study for the structure of fibrin networks in the clots of blood and plasma. *Biorheology*. 6:329–339.

Kaibara, M., and E. Fukada. 1971. The influence of the concentration of thrombin and the dynamic viscoelasticity of clotting blood and fibrinogen-thrombin systems. *Biorheology.* 8:139–147.

Kang, E. P., and D. C. Triantaphyllopoulos. 1977a. Fibrin digestion by thrombin. Comparison with plasmin-digested fibrinogen. *Biochim. Biophys. Acta*. 490:403–442.

Kang, E. P., and D. C. Triantaphyllopoulos. 1977b. Fibrin digestion by thrombin. The significance of the arginyl and lysyl bonds. *Thromb. Res.* 11:403–415.

Kaplan, E. L., and P. Meier. 1958. Nonparametric estimation from incomplete observations. *J. Am. Stat. Assoc.* 53:457–481.

Kolev, K., K. Tenekedjiev, E. Komorowicz, and R. Machovich. 1997. Functional evaluation of the structural features of proteases and their substrate in fibrin surface degradation. *J. Biol. Chem*. 272: 13606–13675.

Laemmli, U. K. 1970. Cleavage of structural proteins during the assembly of the head of bacteriophage T4. *Nature (Lond.).* 227:680–685.

Langer, B. G., J. W. Weisel, P. A. Dinauer, C. Nagaswami, and W. R. Bell. 1988. Deglycosylation of fibrinogen accelerates polymerization and increases lateral aggregation of fibrin fibers. *J. Biol. Chem.* 263: 15056–15063.

Laudano, A. P., and R. F. Doolittle. 1981. Influence of calcium ion on the binding of fibrin amino terminal peptides to fibrinogen. *Science (Wash. DC).* 212:457–459.

Lorand, L., and K. Konishi. 1964. Activation of the fibrin stabilization factor of plasma by thrombin. *Arch. Biochem. Biophys.* 105:58–67.

Lorand, L., N. G. Rule, H. H. Ong, R. Furlanetto, A. Jacobsen, J. Downey, N. Oner, and J. Bruner-Lorand. 1968. Amine specificity in transpeptidation. Inhibition of fibrin cross-linking. *Biochemistry.* 7:1214–1223.

Mark, J. E. 1982. Experimental determinations of crosslink densities. *Rubber Chem. Technol.* 55:762–768.

Marx, G. 1988. Elasticity of fibrin and protofibrin gels is differentially modulated by calcium and zinc. *Thromb. Haemostasis.* 59:500–503.

Matacic, S., and A. G. Loewy. 1968. The identification of isopeptide cross-links in insoluble fibrin. *Biochem. Biophys. Res. Commun.* 30: 356–362.

McKee, P. A., P. Mattock, and R. L. Hill. 1970. Subunit structure of human fibrinogen, soluble fibrin, and cross-linked insoluble fibrin. *Proc. Natl. Acad. Sci. USA.* 66:738–744.

Mihalyi, E. 1968. Physicochemical studies of bovine fibrinogen. IV. Ultraviolet absorption and its relation to the structure of the molecule. *Biochemistry.* 7:208–223.

Mihalyi, E. 1988. Clotting of bovine fibrinogen. Calcium binding to fibrin during clotting and its dependence on release of fibrinopeptide B. *Biochemistry.* 27:967–976.

Mockros, L. F., W. W. Roberts, and L. Lorand. 1974. Viscoelastic properties of ligation-inhibited fibrin clots. *Biophys. Chem.* 2:164–169.

Mosesson, M. W., J. P. DiOrio, K. R. Siebenlist, J. S. Wall, and J. F. Hainfeld. 1993. Evidence for a second type of fibril branch point in fibrin polymer networks, the trimolecular junction. *Blood.* 82: 1517–1521.

Mosesson, M. W., K. R. Siebenlist, D. L. Amrani, and J. P. DiOrio. 1989. Identification of covalently linked trimeric and tetrameric D domains in cross-linked fibrin. *Proc. Natl. Acad. Sci. USA.* 86:1113–1117.

Muller, M. F., H. Ris, and J. D. Ferry. 1984. Electron microscopy of fine fibrin clots and fine and coarse fibrin films. Observations of fibers in cross-section and in deformed states. *J. Mol. Biol.* 174:369–384.

Murthy, S. N. P., and L. Lorand. 1990. Cross-linked A$\alpha\gamma$ chain hybrids serve as unique markers for fibrinogen polymerized by tissue transglutaminase. *Proc. Natl. Acad. Sci. USA.* 87:9679–9682.

Nelb, G. W., C. Gerth, J. D. Ferry, and L. Lorand. 1976. Rheology of fibrin clots. III. Shear creep and creep recovery of fine ligated and coarse unligated clots. *Biophys. Chem.* 5:377–387.

Nelb, G. W., G. W. Kamykowski, and J. D. Ferry. 1981. Rheology of fibrin clots. V. Shear modulus, creep, and creep recovery of fine unligated clots. *Biophys. Chem.* 13:15–23.

Okada, M., and B. Blomback. 1983. Calcium and fibrin gel structure. *Thromb. Res.* 29:269–280.

Pisano, J. J., J. S. Finlayson, and M. P. Peyton. 1968. Cross-link in fibrin polymerized by factor XIII: ϵ(γ-glutamyl)lysine. *Science (Wash. DC).* 160:892–893.

Ratnoff, O. D., and A. M. Potts. 1954. Accelerating effect of calcium and other cations on conversion of fibrinogen to fibrin. *J. Clin. Invest.* 33:206–210.

Roberts, W. W., O. Kramer, R. W. Rosser, F. H. M. Nestler, and J. D. Ferry. 1974. Rheology of fibrin clots. I. Dynamic viscoelastic properties and fluid permeation. *Biophys. Chem.* 1:152–160.

Roberts, W. W., L. L. Lorand, and L. F. Mockros. 1973. Viscoelastic properties of fibrin clots. *Biorheology.* 10:29–42.

Rosenfeld, G., and B. Janszky. 1952. Accelerating effect of calcium on the fibrinogen-fibrin transformation. *Science (Wash. DC).* 116:36–37.

Rosser, R. W., W. W. Roberts, and J. D. Ferry. 1977. Rheology of fibrin clots. IV. Darcy constants and fiber thickness. *Biophys. Chem.* 7:153–157.

Schwartz, M. L., S. V. Pizzo, R. L. Hill, and P. A. McKee. 1971. The effect of fibrin-stabilizing factor on the subunit structure of human fibrin. *J. Clin. Invest.* 50:1506–1513.

Scrutton, M. C., S. B. Ross-Murphy, G. M. Bennett, Y. Stirling, and T. W. Meade. 1994. Changes in clot deformability—a possible explanation for the epidemiological association between plasma fibrinogen concentration and myocardial infarction. *Blood Coagul. Fibrinolysis.* 5:719–723.

Shah, G. A., C. H. Nair, and D. P. Dhall. 1985. Physiological studies on fibrin network structure. *Thromb. Res.* 40:181–188.

Shainoff, J. R., D. A. Urbanic, and P. M. DiBello. 1991. Immunoelectrophoretic characterizations of the cross-linking of fibrinogen and fibrin by factor XIIIa and tissue transglutaminase. *J. Biol. Chem.* 266:6429–6437.

Shen, L. L., J. Hermans, J. McDonagh, R. P. McDonagh, and M. Carr. 1975. Effects of calcium ion and covalent cross-linking on formation and elasticity of fibrin gels. *Thromb. Res.* 6:255–256.

Shen, L. L., and L. Lorand. 1983. Contribution of fibrin stabilization to clot strength. Supplementation of factor XIII-deficient plasma with the purified zymogen. *J. Clin. Invest.* 71:1336–1341.

Shen, L. L., R. P. McDonagh, J. McDonagh, and J. Hermans. 1974. Fibrin gel structure: influence of calcium and covalent cross-linking on the elasticity. *Biochem. Biophys. Res. Commun.* 56:793–799.

Siebenlist, K. R., and M. W. Mosesson. 1992. Factors affecting γ-chain multimer formation in cross-linked fibrin. *Biochemistry.* 31:936–941.

Sobel, J. H., C. A. Thibodeau, and R. E. Canfield. 1988. Early alpha chain cross-linking in human fibrin preparations. *Thromb. Haemostasis.* 60: 153–159.

Triantaphyllopoulos, D. C., and S. Chandra. 1973. Digestion of fibrin by thrombin. *Biochim. Biophys. Acta.* 328:229–232.

Veklich, Y. I., O. V. Gorkun, L. V. Medved, W. Nieuwenhuizen, and J. W. Weisel. 1993. Carboxyl-terminal portions of the α chains of fibrinogen and fibrin. *J. Biol. Chem.* 268:1–9.

Weisel, J. W., and C. Nagaswami. 1992. Computer modeling of fibrin polymerization kinetics correlated with electron microscope and turbidity observations: clot structure and assembly are kinetically controlled. *Biophys. J.* 63:111–128.

Weisel, J. W., C. V. Stauffacher, E. Bullitt, and C. Cohen. 1985. A model for fibrinogen: domains and sequence. *Science (Wash. DC).* 230: 1388–1391.

Weisel, J. W., Y. Veklich, and O. Gorkun. 1993. The sequence of cleavage of fibrinopeptides from fibrinogen is important for protofibril formation and enhancement of lateral aggregation in fibrin clots. *J. Mol. Biol.* 232:285–297.

Wolfe, J. K., and D. F. Waugh. 1981. Relations between enzymatic and association reactions in the development of bovine fibrin clot structure. *Arch. Biochem. Biophys.* 211:125–142.